

A giant planet orbiting the 'extreme horizontal branch' star V 391 Pegasi

R. Silvotti¹, S. Schuh², R. Janulis³, J.-E. Solheim⁴, S. Bernabei⁵, R. Østensen⁶, T. D. Oswalt⁷, I. Bruni⁵, R. Gualandi⁵, A. Bonanno⁸, G. Vauclair⁹, M. Reed¹⁰, C.-W. Chen¹¹, E. Leibowitz¹², M. Paparo¹³, A. Baran¹⁴, S. Charpinet⁹, N. Dolez⁹, S. Kawaler¹⁵, D. Kurtz¹⁶, P. Moskalik¹⁷, R. Riddle¹⁸ & S. Zola^{14,19}

After the initial discoveries fifteen years ago^{1,2}, over 200 extrasolar planets have now been detected. Most of them orbit main-sequence stars similar to our Sun, although a few planets orbiting red giant stars have been recently found³. When the hydrogen in their cores runs out, main-sequence stars undergo an expansion into red-giant stars. This expansion can modify the orbits of planets and can easily reach and engulf the inner planets. The same will happen to the planets of our Solar System in about five billion years and the fate of the Earth is matter of debate^{4,5}. Here we report the discovery of a planetary-mass body ($M\sin i = 3.2M_{\text{Jupiter}}$) orbiting the star V 391 Pegasi at a distance of about 1.7 astronomical units (AU), with a period of 3.2 years. This star is on the extreme horizontal branch of the Hertzsprung–Russell diagram, burning helium in its core and pulsating. The maximum radius of the red-giant precursor of V 391 Pegasi may have reached 0.7 AU, while the orbital distance of the planet during the stellar main-sequence phase is estimated to be about 1 AU. This detection of a planet orbiting a post-red-giant star demonstrates that planets with orbital distances of less than 2 AU can survive the red-giant expansion of their parent stars.

With an effective temperature close to 30,000 K and a surface gravity ten times that of the Sun⁶, V 391 Pegasi (or HS 2201+2610 from the original Hamburg Schmidt survey name) is one of about 40 hot subdwarf B stars showing short-period p-mode pulsations⁷. Its pulsational spectrum exhibits four or five pulsation periods^{6,8} between 342 and 354 s (see Supplementary Information for more details on the star's properties).

Because of their compact structure, subdwarf B pulsators have extremely stable oscillation periods, like white dwarf pulsators. It is therefore possible to register very small differences in the arrival times of the photons^{9,10}, which in principle allows the detection of low-mass secondary bodies¹¹, through the use of the observed–calculated (O–C) diagram¹² (see Fig. 1 legend for more details). Functionally, it is equivalent to the timing method used to find planets around pulsars^{1,13}.

When a pulsation period changes linearly in time, the O–C diagram has a parabolic shape, as confirmed by all the previous measurements of dP/dt (or \dot{P}) in compact pulsators^{9,14,15}. The same behaviour is found in the O–C plot of V 391 Peg (upper panel of

Fig. 1), implying that the main pulsation period of the star is increasing at a rate of $\dot{P}_1 = (1.46 \pm 0.07) \times 10^{-12}$ (or 1 s in 22,000 years).

For V 391 Peg a simple second-order polynomial does not give a satisfactory fit and the sinusoidal residuals require further interpretation (lower panel of Fig. 1). An oscillating \dot{P} is not compatible with any evolutionary or pulsational model: it would require that the star expands and contracts periodically every 3 years, a time much larger than the dynamical timescale, which is of the order of 500 s for a subdwarf B star. Nor can the sinusoidal residuals be explained by any known pulsational effect. Random period variations¹⁶ are also not a possibility because these variations would be cancelled by the large number of pulsation cycles (>28 for each point in Fig. 1).

The simplest explanation for the sinusoidal component of the O–C diagram in Fig. 1 is a wobble of the star's barycentre due to the presence of a low-mass companion. Depending on its position around the barycentre of the system, the subdwarf B star is periodically closer to, or more distant from us by 5.3 ± 0.6 light seconds and the timing of the pulsation is cyclically advanced or delayed. From our best fit and Kepler's third law (assuming a circular orbit, $M_1 = 0.5M_{\text{Sun}}$, where M_{Sun} is the mass of the Sun, and $M_2 \ll M_1$), we obtain: $P_{\text{orb}} = 1,170 \pm 44$ days (or 3.20 ± 0.12 years), $a = 1.7$ AU and $M_2\sin i = 3.2M_{\text{Jupiter}}$, where a is the planet–star separation and 1 AU is the mean distance between the Earth and the Sun. The orbital parameters of the system are listed in Table 1. This interpretation is robust: the

Table 1 | Orbital parameters

Parameter	Value
Orbital period, P_{orb} (d)	$1,170 \pm 44$
Epoch of maximum time delay, T_0 (BJD)	$2,452,418 \pm 96$
Eccentricity, e (assumed)	0.0
Star projected orbital radius, $a_s\sin i$ (km)	$1,600,000 \pm 190,000$
Star projected orbital velocity, $v_s\sin i$ (m s^{-1})	99 ± 12
Mass function*, $f(M_1, M_2)$ (M_{Sun})	$(1.19 \pm 0.43) \times 10^{-7}$
Distance from the star†, a (AU)	1.7 ± 0.1
Maximum elongation† (milliarcsec)	1.2 ± 0.1
Planet orbital velocity†, v_p (km s^{-1})	16 ± 1
Planet mass†, $M_2\sin i$ (M_{Jupiter})	3.2 ± 0.7

$$* f(M_1, M_2) = 4\pi^2 (a_s \sin i)^3 / GP_{\text{orb}}^2 = (M_2 \sin i)^3 / (M_1 + M_2)^2.$$

† These numbers are obtained assuming $M_1 = 0.5 \pm 0.05M_{\text{Sun}}$ (suggested from asteroseismology) and $M_2 \ll M_1$.

¹INAF-Osservatorio Astronomico di Capodimonte, via Moiriello 16, 80131 Napoli, Italy. ²Institut für Astrophysik, Universität Göttingen, Friedrich-Hund-Platz 1, 37077 Göttingen, Germany. ³Institute of Theoretical Physics and Astronomy, Vilnius University, 12 A. Gostauto Street, 01108 Vilnius, Lithuania. ⁴Institut for Teoretisk Astrofysikk, Universitetet i Oslo, PB 1029 Blindern, 0315, Norway. ⁵INAF-Osservatorio Astronomico di Bologna, via Ranzani 1, 40127 Bologna, Italy. ⁶K. U. Leuven, Institute of Astronomy, Celestijnenlaan 200D, 3001 Leuven, Belgium. ⁷Department of Physics and Space Sciences and the SARA Observatory, Florida Institute of Technology, 150 West University Boulevard, Melbourne, Florida 32901, USA. ⁸INAF-Osservatorio Astrofisico di Catania, via S. Sofia 78, 95123 Catania, Italy. ⁹CNRS-UMR5572, Observatoire Midi-Pyrénées, Université Paul Sabatier, 14 avenue Edouard Belin, 31400 Toulouse, France. ¹⁰Department of Physics, Astronomy and Materials Science, Missouri State University, 901 S. National, Springfield, Missouri 65897, USA. ¹¹Institute of Astronomy, National Central University, 300 Jhongda Road, Chung-Li 32054, Taiwan. ¹²Wise Observatory, Tel Aviv University, Tel Aviv 69978, Israel. ¹³Konkoly Observatory, P O Box 67, H-1525 Budapest XII, Hungary. ¹⁴Cracow Pedagogical University, ul. Podchorążych 2, 30-084 Cracow, Poland. ¹⁵Department of Physics and Astronomy, 12 Physics Hall, Iowa State University, Ames, Iowa 50011, USA. ¹⁶Centre for Astrophysics, University of Central Lancashire, Preston PR1 2HE, UK. ¹⁷Copernicus Astronomical Centre, ul. Bartycka 18, 00-716 Warsaw, Poland. ¹⁸Thirty Meter Telescope Project, 2632 E. Washington Blvd, Pasadena, California 91107, USA. ¹⁹Astronomical Observatory, Jagiellonian University, ul. Orla 171, 30-244 Cracow, Poland.

same sinusoidal component is also found in the O–C diagram of the secondary pulsation frequency of the star (see Figs 2 and 3 for more details). Any alternative interpretation of our results would have to be compatible with this fact. The sinusoids in the lower panels of Figs 1, 2 and 3 suggest a circular orbit. From our observations we cannot yet set a precise upper limit to the eccentricity, but it must be close to zero.

Using the known characteristics of the V 391 Peg system, we can determine a first estimate of the planet's effective temperature by balancing the flux received from the star with the blackbody flux re-radiated by the planet (see Supplementary Information for more details). Assuming a Bond albedo of 0.343 (similar to that of Jupiter¹⁷), we obtain an effective temperature for the planet of about 470 K, corresponding to a maximum of the blackbody radiation near 6.2 μm from Wien's law.

With a projected radius of about five light seconds, the wobble of the barycentre of V 391 Peg points towards a planet (for comparison, the amplitude of the solar displacement around the barycentre of our Solar System is almost three light seconds). However, depending on the unknown inclination i of the system, a brown dwarf or even a low-mass stellar companion cannot be totally excluded. But the low inclination required ($2.5^\circ \leq i \leq 14^\circ$ for a brown dwarf or $i \leq 2.5^\circ$ for a low-mass stellar companion) has a very low probability (3%

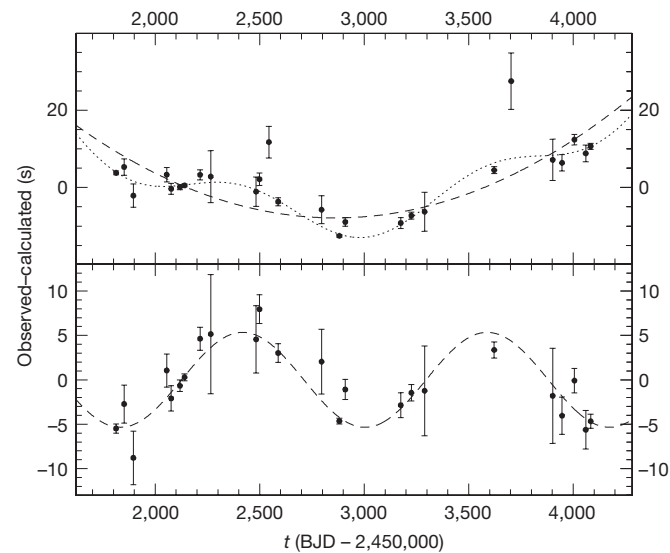


Figure 1 | The O–C diagram of the main pulsation frequency f_1 of V 391 Peg. The O–C technique is a way of measuring the phase variations of a periodic function, comparing the observed times of the maxima with those calculated from an ephemeris¹². In our case, what is compared is the time of the first maximum of each single run (obtained by fitting the data with five sinusoids simultaneously, corresponding to the five pulsation frequencies) with the best ephemeris obtained fitting the whole (seven-year-long) data set. The error bars are given by $(\sigma_o^2 + \sigma_c^2)^{1/2}$, where σ_o and σ_c are the 1σ phase errors obtained from the least-squares sinusoidal fits. The upper panel shows that the fit of the long-term component by a second-order polynomial is significantly improved when we also use a sine wave. Fitting the data with both functions simultaneously reduces the value of the reduced χ^2 from 14.1 (second-order polynomial alone) to 2.7. The lower panel shows the sinusoidal component alone. To obtain these plots, 418 h of time-series photometry from 167 nights of observation were used, from 18 different 1-m to 3-m class telescopes (see Supplementary Information for more details). The number of photometric measurements for each point varies from 237 (the highest point with large error bar) to 26,081 (the first point on the left). In total, the number of photometric measurements is 109,531. The data were reduced following standard procedures for time-series photometry, using statistical weights²⁷ and barycentric time corrections²⁸ (BJD stands for barycentric Julian day). One second was added to the data of 2006 only, to compensate for the leap-second correction of 1 January 2006. Looking at the time distribution of the phase measurements, we note that there are seven groups of close points corresponding to the seven observing seasons (from May to December) of the last seven years (2000 to 2006).

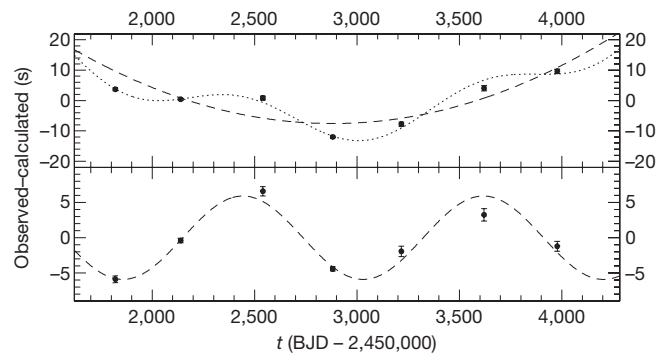


Figure 2 | The O–C diagram of f_1 . In this version of the O–C diagram, all the runs of each observing season were combined and the phases were recalculated on these larger data sets. This reduces the noise (but also reduces the time resolution), so that in principle O–C diagrams can be built for each pulsation frequency of a multiperiodic pulsator. In this way, if the pulsating star has a companion, each pulsation mode can supply an independent confirmation of the periodic motion around the centre of mass. V 391 Peg has four or five pulsation periods; for the two that have sufficiently large amplitudes of 1% and 0.4% respectively, O–C diagrams can be obtained. As in Fig. 1, the upper and lower plots represent respectively the O–C diagram of f_1 and its sinusoidal component alone. The error bars are calculated as in Fig. 1.

and 0.1% respectively), assuming a random distribution of orbital plane inclinations.

Thus, with a 97% probability, V 391 Peg b is the first recognized planet orbiting a post-red-giant star, making this system a unique laboratory in which to test the evolution of planetary systems during and after the red-giant expansion. With a probable age of the order of 10 Gyr (see Supplementary Information for more details), V 391 Peg b is also one of the oldest planets known. An interesting case of a brown dwarf that survived engulfment by a red giant was recently presented¹⁸; the information about whether low-mass companions to red-giant stars survive engulfment in that system is complementary to that of V 391 Peg, because the two systems are very different. We note that only by studying planets of horizontal branch stars is it possible to

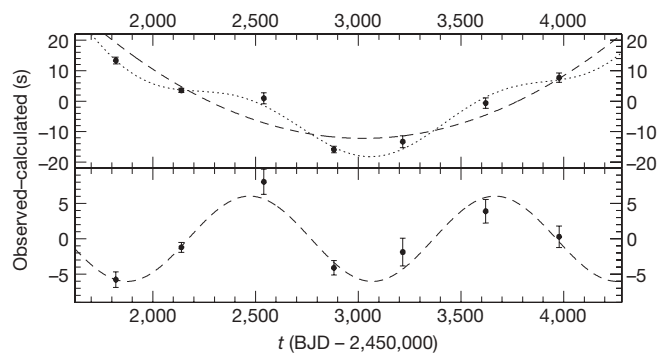


Figure 3 | The O–C diagram of f_2 . As for Fig. 2 but relative to the second pulsation frequency f_2 . Comparing the lower panels of Figs 2 and 3, we see that the two sinusoids of f_1 and f_2 are identical within the errors. The agreement between periods, amplitudes and phases is always better than 0.2σ . We obtain respectively $1,174 \pm 94$ days versus $1,194 \pm 106$ days, 5.9 ± 1.6 s versus 6.0 ± 2.3 s, and $\text{BJD } 2,452,443 \pm 194$ versus $\text{BJD } 2,452,471 \pm 211$ for the epoch of the first maximum. From the second-order polynomial component of the fit in the upper panel, we obtain also a measurement of the secular variation of f_2 : $\dot{P}_2 = (2.05 \pm 0.26) \times 10^{-12}$, which is different from $\dot{P}_1 = (1.46 \pm 0.07) \times 10^{-12}$. The absolute values of \dot{P}_1 and \dot{P}_2 , which correspond to an evolutionary timescale P/\dot{P} of 7.6×10^6 and 5.5×10^6 years respectively, match relatively well with theoretical expectations for evolved models of extreme horizontal branch stars²⁹ (even though their positive sign is more difficult to explain and suggests that the star is expanding, as confirmed by some tests done by one of us). We note that the difference between \dot{P}_1 and \dot{P}_2 excludes the possibility that the long-term component of the O–C plots is due to a secondary planet with a larger orbit. The error bars are calculated as in Fig. 1.

isolate the effects of the red-giant expansion on a planetary system. Planets around white dwarfs must be strongly modified also by the asymptotic giant branch expansion, the thermal pulses and the final planetary nebula ejection¹⁹.

Even though, in terms of orbit stability, the existence of V 391 Peg b is not surprising²⁰, in terms of orbit evolution during the red-giant phase, the situation is less clear. There are at least two competing processes that determine the orbital evolution: mass loss from the star that causes the orbit of a planet to expand, and tidal effects that tend to reduce its angular momentum causing spiralling-in²¹. Neither the stellar mass loss nor the tidal dissipation are well-understood processes. For this reason, the destiny of our Earth is still a matter of debate^{4,5}. For V 391 Peg b the most likely scenario is that the planet never entered the stellar envelope (the maximum radius expected for a subdwarf B progenitor at the tip of the red-giant branch^{22,23} is of the order of 0.7 AU) and that the orbit of V 391 Peg b was tighter in the past owing to the strong mass loss of the parent star, with an orbital radius of about 1 AU when the star was still on the main sequence. This value is obtained by assuming that the stellar mass has been reduced from $0.85M_{\text{Sun}}$ to $0.5M_{\text{Sun}}$, when tidal interaction (which is proportional to $(R/r)^8$; ref. 24) can be neglected for a sufficiently large orbital distance r with respect to the stellar radius R . In this scenario the increase of the planet's mass due to accretion from the stellar wind is negligible²⁰. We note that in this case, incidentally, the orbital distances of V 391 Peg b and of the Earth, before and after the red-giant phase, are very similar: 1.5 AU is a reasonable value for the Earth after red-giant migration, when tidal effects are not considered^{4,5}.

A different scenario is obtained if the mass loss of the red-giant precursor of V 391 Peg started sufficiently late: in this case the ratio between stellar radius and orbital distance could have reached a value of about 0.7, at which the star fills its Roche lobe²⁵ and mass transfer to the planet starts, causing the planet to spiral quickly into the outer layers of the giant's atmosphere. Here accretion is disrupted and the spiral-in due to accretion stops, so that the planet may have survived if the spiral-in due to friction was sufficiently low. The presence of planets with orbital separations $\lesssim 5$ AU has been invoked by a few authors to explain the strong mass loss needed to form subdwarf B stars and partially explain the irregular morphology of the horizontal branch²⁶.

Received 6 April; accepted 26 July 2007.

1. Wolszczan, A. & Frail, D. A. A planetary system around the millisecond pulsar PSR1257+12. *Nature* **355**, 145–147 (1992).
2. Mayor, M. & Queloz, D. A Jupiter-mass companion to a solar-type star. *Nature* **378**, 355–359 (1995).
3. Döllinger, M. P. *et al.* Discovery of a planet around the K giant star 4 U Ma. *Astron. Astrophys.* (in the press); preprint at (<http://arxiv.org/astro-ph/0703672>).
4. Rasio, F. A., Tout, C. A., Lubow, S. H. & Livio, M. Tidal decay of close planetary orbits. *Astrophys. J.* **470**, 1187–1191 (1996).
5. Rybicki, K. R. & Denis, C. On the final destiny of the Earth and the Solar System. *Icarus* **151**, 130–137 (2001).
6. Østensen, R. *et al.* Detection of pulsations in three subdwarf B stars. *Astron. Astrophys.* **368**, 175–182 (2001).
7. Kilkeny, D. Pulsating hot subdwarfs—an observational review. *Commun. Asteroseismol.* **150**, 234–240 (2007).
8. Silvotti, R. *et al.* The temporal spectrum of the sdB pulsating star HS 2201+2610 at 2 ms resolution. *Astron. Astrophys.* **389**, 180–190 (2002).
9. Kepler, S. O. *et al.* Measuring the evolution of the most stable optical clock G 117–B15A. *Astrophys. J.* **634**, 1311–1318 (2005).
10. Reed, M. *et al.* Observations of the pulsating subdwarf B star Feige 48: constraints on evolution and companions. *Mon. Not. R. Astron. Soc.* **348**, 1164–1174 (2004).

11. Winget, D. E. *et al.* The search for planets around pulsating white dwarf stars. *ASP Conf. Ser.* **294**, 59–64 (2003).
12. Sterken, C. The O–C diagram: basic procedures. *ASP Conf. Ser.* **335**, 3–23 (2005).
13. Thorsett, S. E., Arzoumanian, Z. & Taylor, J. H. PSR B1620–26—A binary radio pulsar with a planetary companion? *Astrophys. J.* **412**, L33–L36 (1993).
14. Costa, J. E. S., Kepler, S. O. & Winget, D. E. Direct measurement of a secular pulsation period change in the pulsating hot pre-white dwarf PG 1159–035. *Astrophys. J.* **522**, 973–982 (1999).
15. Mukadam, A. S. *et al.* Constraining the evolution of ZZ Ceti. *Astrophys. J.* **594**, 961–970 (2003).
16. Koen, C. Statistics of O–C diagrams and period changes. *ASP Conf. Ser.* **335**, 25–35 (2005).
17. Hanel, R., Conrath, B., Herath, L., Kunde, V. & Pirraglia, J. Albedo, internal heat, and energy balance of Jupiter—preliminary results of the Voyager infrared investigation. *J. Geophys. Res.* **86**, 8705–8712 (1981).
18. Maxted, P. F. L., Napiwotzki, R., Dobbie, P. D. & Burleigh, M. R. Survival of a brown dwarf after engulfment by a red giant star. *Nature* **442**, 543–545 (2006).
19. Villaver, E. & Livio, M. Can planets survive stellar evolution? *Astrophys. J.* **661**, 1192–1201 (2007).
20. Duncan, M. J. & Lissauer, J. J. The effects of post-main-sequence solar mass loss on the stability of our planetary system. *Icarus* **134**, 303–310 (1998).
21. Livio, M. & Soker, N. Star-planet systems as progenitors of cataclysmic binaries: tidal effects. *Astron. Astrophys.* **125**, L12–L15 (1983).
22. Sweigart, A. V. & Gross, P. G. Evolutionary sequences for red giant stars. *Astrophys. J.* **36** (Suppl.), 405–437 (1978).
23. Han, Z., Podsiadlowski, Ph., Maxted, P. F. L., Marsh, T. R. & Ivanova, N. The origin of subdwarf B stars—I. The formation channels. *Mon. Not. R. Astron. Soc.* **336**, 449–466 (2002).
24. Zahn, J. P. Tidal friction in close binary stars. *Astron. Astrophys.* **57**, 383–394 (1977).
25. Eggleton, P. P. Approximations to the radii of Roche lobes. *Astrophys. J.* **268**, 368–369 (1983).
26. Soker, N. Can planets influence the horizontal branch morphology? *Astron. J.* **116**, 1308–1313 (1998).
27. Silvotti, R. *et al.* The rapidly pulsating subdwarf B star PG 1325+101. I. Oscillation modes from multisite observations. *Astron. Astrophys.* **459**, 557–564 (2006).
28. Stumpff, P. Two self-consistent FORTRAN subroutines for the computation of the Earth's motion. *Astron. Astrophys. Suppl. Ser.* **41**, 1–8 (1980).
29. Charpinet, S., Fontaine, G., Brassard, P. & Dorman, B. Adiabatic survey of subdwarf B star oscillations. III. Effects of extreme horizontal branch stellar evolution on pulsation modes. *Astrophys. J.* **140** (Suppl.), 469–561 (2002).

Supplementary Information is linked to the online version of the paper at www.nature.com/nature.

Acknowledgements R.S. thanks M. Capaccioli, J. M. Alcalá, E. Covino and S. O. Kepler for discussions and suggestions, S. Marinoni and S. Galletti for their contribution to the observations, and the MiUR for financial support. S.S. thanks T. Nagel, E. Goehler, T. Stahn, S. D. Huegelmeier, R. Lutz, U. Thiele and A. Guizarro for their help in data acquisition, and the DFG for travel grants. R.Ø. is supported by the Research Council of the University of Leuven and by the FP6 Coordination Action HELAS of the EU. T.D.O. acknowledges support from the US National Science Foundation. P.M. acknowledges support from the Polish MNiSW.

Author Contributions R.S. analysed and interpreted the data from which the presence of the planet was inferred. R.S., S.S., R.J., J.-E.S., S.B., R.Ø., T.D.O., I.B., R.G., A. Bonanno, G.V., M.R., C.-W.C., E.L. and M.P. contributed to the large amount of observations and/or data reduction. A. Baran, S.C., N.D., S.K., D.K., P.M., R.R. and S.Z. contributed to the organization and/or on-line data reduction/analysis during the XCov23 Whole Earth Telescope campaign of August–September 2003, in which V 391 Peg was observed as a secondary target. S.K. performed some tests on theoretical P . S.K. and S.Z. did independent checks of the O–C fits. E.L. made statistical tests on the significance level of the O–C fits. All authors discussed and interpreted the results and commented on the manuscript. D.K. and R.Ø. in particular helped to improve the text.

Author Information Reprints and permissions information is available at www.nature.com/reprints. The authors declare no competing financial interests. Correspondence and requests for materials should be addressed to R.S. (silvotti@na.astro.it).